

Low-Temperature Crystallization and Highly Enhanced Photoluminescence of $\text{Gd}_{2-x}\text{Y}_x\text{O}_3:\text{Eu}^{3+}$ by Li Doping

Song-Ho Byeon,^{†,*} Mi-Gyeong Ko,[†] Jung-Chul Park,[‡] and Dong-Kuk Kim[§]

College of Environment and Applied Chemistry, Institute of Natural Sciences, Kyung Hee University, Kyung Ki 449-701, Korea, Department of Chemistry of New Materials, Silla University, Pusan 617-736, Korea, and Department of Chemistry, College of Natural Sciences, Kyungpook National University, Taegu 702-701, Korea

Received June 1, 2001. Revised Manuscript Received November 5, 2001

The influence of Li doping on the crystallization behavior, morphology, and enhancement in photoemission intensity of $\text{Gd}_{2-x}\text{Y}_x\text{O}_3:\text{Eu}^{3+}$ solid-solution was investigated. To maximize an effect of the Li component which is volatile at elevated temperature, the citrate route was adopted for the synthesis at low temperature (650–850 °C). Firing the metal citrate precursor at 650 °C for 5 h was sufficient for the formation of 100 nm sized, nonaggregated, and spherical Li-doped $\text{Gd}_{2-x}\text{Y}_x\text{O}_3:\text{Eu}^{3+}$ particles, whose photoluminescence (PL) emission intensity is comparable with that of commercial red phosphor $\text{Y}_2\text{O}_3:\text{Eu}^{3+}$. Such a temperature is much lower than the typical solid-state reaction or spray pyrolysis temperature (>1400 °C). Additional heat treatment up to 850 °C resulted in well-developed 500 nm sized pseudospherical particles whose PL brightness is close to ~150% in comparison with that of commercial red phosphor. Li-doped $\text{Gd}_{2-x}\text{Y}_x\text{O}_3:\text{Eu}^{3+}$ appears to be a very promising red phosphor because the particle size and shape can be controlled at low temperature (650–850 °C) by the change of Y or Li contents without significant loss of brightness.

Introduction

Many phosphor materials generate visible light in fluorescent lamps and emissive displays. Excitation of photoluminescent phosphors takes place using ultraviolet (UV) photons generated by a discharge in fluorescent lamp or plasma display panel (PDP).¹ Cathodoluminescence, thermoluminescence, and electroluminescence of phosphors are also important for cathode ray tube (CRT), field emission display (FED), radiation detector, and electroluminescence display (ELD) applications.^{2–6} An improved performance of displays and lamps requires high quality of phosphors for sufficient brightness and long-term stability. Small spherical phosphor particles should be easily processed into smaller pixels and naturally desirable for high-resolution screens, displays, and flat panels. In practice, a densely packed layer of small size particles can improve aging problems. On the other hand, when the particle is smaller than a critical value, the luminescence efficiency decreases because of increased light reabsorption and the luminescence quenching by the

surface layer.⁷ Therefore, the morphology and size, the stoichiometry and composition, and the surface characteristics must be controlled in order to achieve the desirable objectives of improved powder phosphors.

Yttrium oxide and gadolinium oxide doped with Eu^{3+} exhibit strong UV and cathode ray excited luminescences which are useful in lamp and display applications, respectively.^{1,7} $\text{Y}_2\text{O}_3:\text{Eu}^{3+}$ and $\text{Gd}_2\text{O}_3:\text{Eu}^{3+}$ are also used as composite compositions to improve the luminescent properties.⁸ In addition, $(\text{Y,Gd})_2\text{O}_3:\text{Eu}^{3+}$ is a very efficient X-ray and thermoluminescent phosphor.⁹ Preparation of this solid-solution by the conventional method employs a solid-state reaction at high temperatures with sequential grinding and firing steps. This process has disadvantages in maintaining the uniformity of composition and improving the morphology, size, and size distribution of phosphor particles. Spray pyrolysis may be one of available processes to induce spherical morphology, fine size, and narrow size distribution.^{10,11} However, high temperature is also required for the pyrolysis, and the resulting particles are frequently hollow because of fast evaporation of solvent from droplet surface. Various preparation routes have been adopted to reduce the reaction temperature and obtain high-quality small particle size of phosphors.^{2,4,5,12}

[†] Kyung Hee University.

[‡] Silla University.

[§] Kyungpook National University.

* To whom all correspondence should be addressed.

(1) Blasse, G.; Grabmaier, B. C. *Luminescent Materials*; Springer: Berlin, 1994.

(2) Yan, M. F.; Huo, T. C. D.; Ling, H. C. *J. Electrochem. Soc.* **1987**, *134*, 493.

(3) Ronda, C. R.; Smets, B. M. J. *J. Electrochem. Soc.* **1989**, *136*, 570.

(4) Shea, L. E.; McKittrick, J.; Lopez, O. A. *J. Am. Ceram. Soc.* **1996**, *79*, 3257.

(5) Ravichandran, D.; Roy, R.; White, W. B. *J. Mater. Res.* **1997**, *12*, 819.

(6) Oshio, S.; Kitamura, K.; Shigeta, T.; Horii, S.; Matsuoka, T.; Tanaka, S.; Kanda, T. *J. Electrochem. Soc.* **1999**, *146*, 392.

(7) Yamamoto, H. *J. SID* **1996**, *4*, 165.

(8) Rossner, W.; Jermann, F.; Ahne, S.; Ostertag, M. *J. Lumin.* **1997**, *72–74*, 708.

(9) Rossner, W. *IEEE Trans. Nucl. Sci.* **1993**, *40*, 376.

(10) Roh, H. S.; Kang, Y. C.; Park, S. B. *J. Colloid Interface Sci.* **2000**, *228*, 195.

(11) Kang, Y. C.; Roh, H. S.; Park, S. B. *J. Electrochem. Soc.* **2000**, *147*, 1601.

(12) Erdei, S.; Roy, R.; Harshe, G.; Juwhari, S.; Agrawal, H. D.; Ainger, F. W.; White, W. B. *Mater. Res. Bull.* **1995**, *30*, 745.

Recently, we have investigated the effect of Li substitution on the luminescent property of SrTiO₃:Pr³⁺ and Gd₂O₃:Eu³⁺.^{13,14} Such studies showed that the addition of the Li component remarkably affects the morphology of particles as well as the photo- and cathodoluminescent efficiency of phosphor. In this work, Li addition to Gd_{2-x}Y_xO₃:Eu³⁺ solid-solution was explored using a citrate pyrolysis at low temperature. This synthesis method could produce spherical particles and effectively control the particle size. Indeed, 100 nm sized, nonaggregated, and spherical Li-doped Gd_{2-x}Y_xO₃:Eu³⁺ particles, whose photoluminescence (PL) intensities are comparable with that of commercial red phosphor Y₂O₃:Eu³⁺, were prepared at only 650 °C. When the firing temperature was increased to 850 °C, the spherical phosphor particles grew up to 500 nm size, and their PL brightness was close to ~150% in comparison with that of commercial red phosphor.

Experimental Section

Gd_{2-x}Y_xO₃:Eu³⁺ (the molar ratio of Eu³⁺ = 0.10) and corresponding Li-doped phosphors (nominal molar ratio of Li⁺ = 0.10) were synthesized by using the citrate pyrolysis method. The *x* value was limited in the range of 0.0 ≤ *x* ≤ 0.8 because PL intensity significantly decreases when *x* ≥ 1.0. The stoichiometric amounts of Gd₂O₃, Y₂O₃, Li₂CO₃, and Eu₂O₃ were dissolved in HNO₃ solution. Several trial and errors led to the optimum amount of added Li₂CO₃ to be 10 mol % (i.e., nominal composition = Li_{0.10}Eu_{0.10}Gd_{1.60}Y_{0.20}O_{2.90}). The citric acid solution (molar ratio of citric acid/metals = 3) was then added. This step yielded complex citrates of corresponding metal ions. After clear solution was formed by uniform stirring, aqueous NH₄OH solution was added into the mixture until the pH of all solutions was adjusted to be 4–5. The precursors containing excess (30% and 100%) amount of Li₂CO₃ were separately prepared to control the shape and size of phosphor particles. The pyrolysis of precursor citrates was carefully carried out with a gas burner, and then dark-gray powder was recovered. An additional firing of this powder at 650 °C for 5 h was needed for the crystallization of Li-doped Gd_{2-x}Y_xO₃:Eu³⁺ phosphor, whose PL intensity is comparable with that of commercial red phosphor Y₂O₃:Eu³⁺. To compare the composition, crystallization, morphology change, and luminescence behaviors at different temperatures, the precursor powder was separately fired at 750 and 850 °C for 5 h.

The quantitative analysis using the inductively coupled plasma (ICP) method was carried out to determine the Li content in this series. The powder X-ray diffraction pattern was recorded on a rotating anode installed diffractometer (18 kW). The Cu Kα radiation used was monochromated by a curved-crystal graphite. Field emission scanning electron microscopy (FE-SEM) was carried out with a Hitachi S-4200 electron microscope operating at 30 kV. Specimens for electron microscope were coated with Pt–Rh for 180 s under vacuum. The PL intensity of phosphors was measured at room temperature using a Hitachi F-4500 spectrophotometer with a xenon flash lamp. The sample loaded on a powder holder provided by Hitachi (the powder samples were not densely packed on this holder) was mounted about 45° to the excitation and source for PL measurement. All samples were analyzed with the same weight, and the same slit was used to measure the excitation and emission spectra. The emission spectra were recorded using maximum excitation wavelength. The excitation spectra were measured at the emission wavelength of 611 nm with maximum intensity. For comparison, the excitation and emission spectra of commercial Y₂O₃:Eu³⁺ supplied by NICHIA Corp. were measured on the same condition.

Table 1. Experimental Lithium Contents (mole/formula unit) in Samples Prepared for Nominal Composition Li_{0.10}Eu_{0.10}Gd_{1.60}Y_{0.20}O_{2.90} at Different Firing Temperatures

added Li content for the synthesis	firing temp (°C)		
	650	750	850
stoichiometric (0.10 mol) Li	0.09(1)	0.02(1)	0.01(1)
30% excess Li	0.13(2)	0.06(1)	0.03(1)
100% excess Li	0.19(1)	0.16(1)	0.12(1)

Results and Discussion

Synthesis and X-ray Diffraction. The citrate pyrolysis can prepare superfine particles of metal oxides because the citric acid easily complexes a number of metal ions.^{15,16} This method has been applied to prepare nanoparticle of metal oxides.¹⁷ The ability of citric acid to chelate metal ions is highly dependent on the solution parameters such as pH, concentration, and temperature. To obtain pure and stable citrate complexes of Li⁺, Gd³⁺, Eu³⁺, and Y³⁺ and to ensure the complete dissociation of citric acid, the solution pH was maintained at 4–5. Although the phosphor particles with poor crystallinity were obtained even at the stage of citrate pyrolysis, their luminescent properties comparable with that of commercial Y₂O₃:Eu³⁺ could be observed after the heat treatment at 650 °C. Nevertheless, such a low reaction temperature is surprising because the solid-solution between Gd₂O₃ and Y₂O₃ is formed above 1400 °C when the typical solid-state reaction or spray pyrolysis methods are adopted.

Elemental analysis using ICP revealed that a considerable loss of the lithium is induced at high temperature due to the evaporation, the amount of lithium loss being proportional to the firing temperature. For instance, firing the sample of nominal composition Li_{0.10}Eu_{0.10}Gd_{1.60}Y_{0.20}O_{2.90} at 850 °C for 5 h resulted in about 90% loss of Li content (Li_{0.01}Eu_{0.10}Gd_{1.60}Y_{0.20}O_{2.855}) when the stoichiometric amount (0.10 mol/formula unit) of Li component was used for the preparation. Because of such a significant loss of Li, an enhanced photoluminescence behavior was not observed for the phosphor prepared using no excess Li at high temperature. A large amount of excess Li component was needed to obtain the composition close to the nominal one. The final lithium contents of some samples prepared for the nominal composition Li_{0.10}Eu_{0.10}Gd_{1.60}Y_{0.20}O_{2.90}, which showed the most intense red emission among Li-doped Gd_{2-x}Y_xO₃:Eu³⁺ series, are summarized in Table 1.

Figure 1 (top) shows the X-ray powder diffraction patterns of Gd₂O₃:Eu³⁺ and Li-doped Gd_{2-x}Y_xO₃:Eu³⁺ as a function of *x* value after the heat treatment at 650 and 850 °C for 5 h. It can be seen that firing the metal citrate precursor at 650 °C is sufficient for the formation of single phase. In the metal citrate sol-gel process, the high degree of mixing of each metal components on an atomic level in the precursor stage is primarily responsible for the significant lowering of formation temperature of Gd_{2-x}Y_xO₃:Eu³⁺. In addition, the large reactive surface area of the precursor powders induced during

(15) Blank, D. H. A.; Kruidhof, H.; Flokstra, J. *J. Phys. D* **1988**, *21*, 226.

(16) Bernasconi, A.; Schilling, A.; Guo, J. D.; Ott, H. R. *Physica C* **1990**, *166*, 393.

(17) Xu, X. L.; Guo, J. D.; Wang, Y. Z. *Mater. Sci. Eng., B* **2000**, *77*, 207.

(13) Hyeon, K.-A.; Byeon, S.-H.; Park, J.-C.; Kim, D.-K.; Suh, K.-S. *Solid State Commun.* **2000**, *115*, 99.

(14) Park, J.-C.; Moon, H.-K.; Kim, D.-K.; Byeon, S.-H.; Kim, B.-C.; Suh, K.-S. *Appl. Phys. Lett.* **2000**, *77*, 2162.

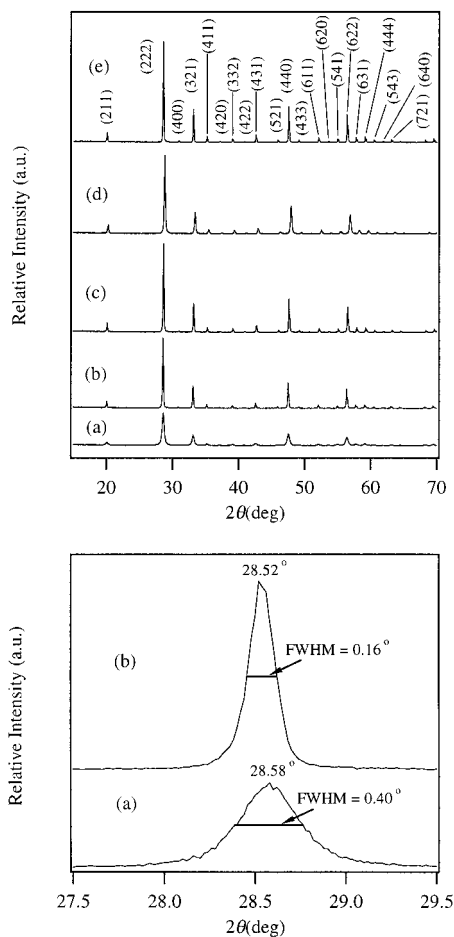


Figure 1. (top) Powder X-ray diffraction patterns of (a) $Gd_2O_3:Eu^{3+}$, (b) Li -doped $Gd_2O_3:Eu^{3+}$, (c) Li -doped $Gd_{1.8}Y_{0.2}O_3:Eu^{3+}$, and (d) Li -doped $Gd_{1.2}Y_{0.8}O_3:Eu^{3+}$ after firing precursor powder at 650 °C for 5 h and (e) Li -doped $Gd_{1.8}Y_{0.2}O_3:Eu^{3+}$ after firing at 850 °C. (bottom) An enlargement of the (222) reflection peak of (a) $Gd_2O_3:Eu^{3+}$ and (b) Li -doped $Gd_2O_3:Eu^{3+}$ after firing at 650 °C for 5 h, showing significantly reduced fwhm after Li doping.

the pyrolysis of metal citrate would also facilitate the rapid crystallization. Since Gd_2O_3 and Y_2O_3 have the same structure of the space group $Ia\bar{3}$,^{18,19} the cubic symmetry is retained in all solid–solution range. When $Gd_2O_3:Eu^{3+}$ is obtained at 650 °C without Li addition, the crystallinity is poor as evidenced by relatively weak and broad X-ray diffraction intensity pattern. In contrast, the diffraction intensities of Li -doped $Gd_2O_3:Eu^{3+}$ are considerably increased due to much better crystallization even after firing at the same temperature. The full width at half-maximum (fwhm) of the (222) peak of Li -doped $Gd_2O_3:Eu^{3+}$ is smaller than one-half in comparison with that of $Gd_2O_3:Eu^{3+}$ before Li doping as shown in Figure 1 (bottom). Furthermore, the (222) peak position shifts slightly toward lower angle upon partial substitution of Li^+ for Gd^{3+} component, indicating an increase in lattice parameter. Occupation of Gd^{3+} sites by Li^+ ions would naturally give rise to a substantial number of vacant sites in the oxygen ion array and then expand the lattice to decrease crystal density. These

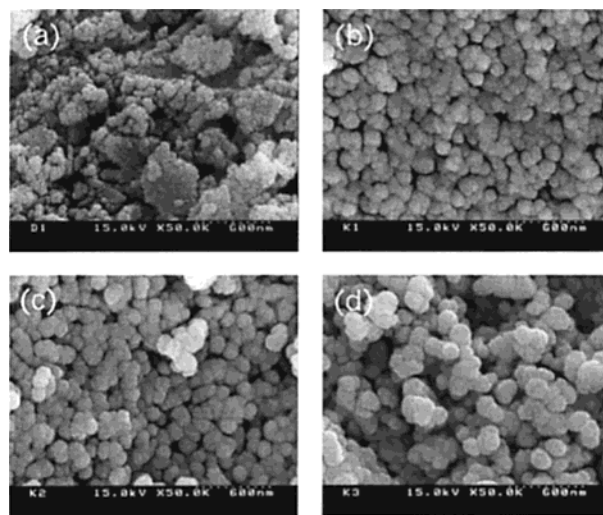


Figure 2. SEM photographs of (a) $Gd_{1.8}Y_{0.2}O_3:Eu^{3+}$ and Li -doped $Gd_{1.8}Y_{0.2}O_3:Eu^{3+}$ after firing at 650 °C for 5 h the precursor powder prepared using (b) stoichiometric, (c) 30% excess, and (d) 100% excess amount of Li component.

X-ray diffraction data imply that the added Li component for the preparation of citrate precursor plays the role to promote effectively an incorporation of Eu_2O_3 and Y_2O_3 into Gd_2O_3 as well as Li itself is incorporated into the host matrix during the firing process. Further increase of heating temperature to 850 °C gives rise to an improved crystallinity of Li -doped $Gd_{2-x}Y_xO_3:Eu^{3+}$ phosphor particles, resulting in the increased PL emission intensity.

Particle Size, Morphology, and Size Distribution. Because the composition of $Gd_{1.8}Y_{0.2}O_3:Eu^{3+}$ exhibits the most intense photoluminescence among $Gd_{2-x}Y_xO_3:Eu^{3+}$ series after Li doping (see the next section), SEM photographs of $Gd_{1.8}Y_{0.2}O_3:Eu^{3+}$ and Li -doped $Gd_{1.8}Y_{0.2}O_3:Eu^{3+}$ prepared by firing the precursor powder at 650 °C for 5 h are compared in Figure 2. It can be seen from SEM images that the growth of $Gd_{1.8}Y_{0.2}O_3:Eu^{3+}$ particles is not sufficient to have any morphology before Li doping (Figure 2a), and in part some agglomerations are observed. In contrast, the particles after Li doping are all spheres, regular, and nonaggregated. Thus, it is evident that the Li coactivators were incorporated into the $Gd_{1.8}Y_{0.2}O_3:Eu^{3+}$ lattice and should serve as a self-promoter for the crystallization and activation even at 650 °C. The mean size of particles prepared using the stoichiometric amount (10 mol %) of Li_2CO_3 are ~ 80 nm (Figure 2b). When 30% and 100% excess amount of Li_2CO_3 are added for the preparation of the citrate precursor, the particles grow to mean size of ~ 100 nm (Figure 2c) and ~ 120 nm (Figure 2d), respectively. Figure 3 shows SEM photographs of $Gd_{1.8}Y_{0.2}O_3:Eu^{3+}$ and Li -doped $Gd_{1.8}Y_{0.2}O_3:Eu^{3+}$ after firing at 750 °C for 5 h. Compared with those fired at 650 °C, the overall particle size significantly increased. While the overall particle shape of $Gd_{1.8}Y_{0.2}O_3:Eu^{3+}$ is never improved before Li doping, the spherical morphology of particles is retained for Li -doped ones. Although a development of particle growth depending on the excess amount of added Li_2CO_3 is not clearly shown in this figure, the worst size distribution is observed when 100% excess of Li_2CO_3 was added.

(18) Buijs, M.; Meyerink, A.; Blasse, G. *J. Lumin.* **1987**, *37*, 9.

(19) Kevorkov, A. M.; Karyagin, V. F.; Munchaev, A. I.; Uyukin, E. M.; Bolotina, N. B.; Chernaya, T. S.; Bagdasarov, K. S.; Simonov, V. I. *Crystallogr. Rep.* **1995**, *40*, 23.

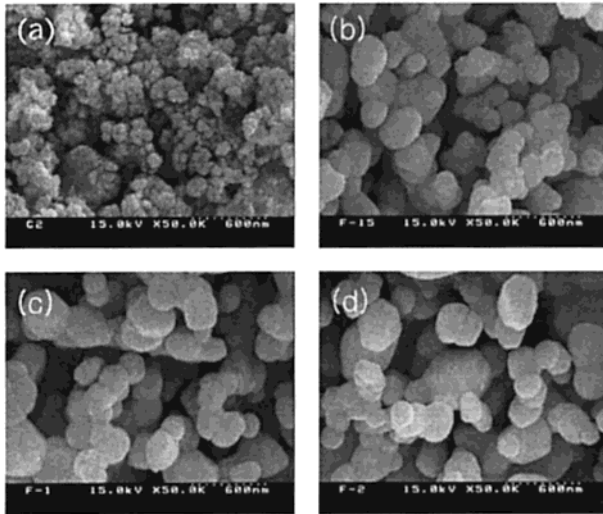


Figure 3. SEM photographs of (a) $\text{Gd}_{1.8}\text{Y}_{0.2}\text{O}_3:\text{Eu}^{3+}$ and Li-doped $\text{Gd}_{1.8}\text{Y}_{0.2}\text{O}_3:\text{Eu}^{3+}$ after firing at 750 °C for 5 h the precursor powder prepared using (b) stoichiometric, (c) 30% excess, and (d) 100% excess amount of Li component.

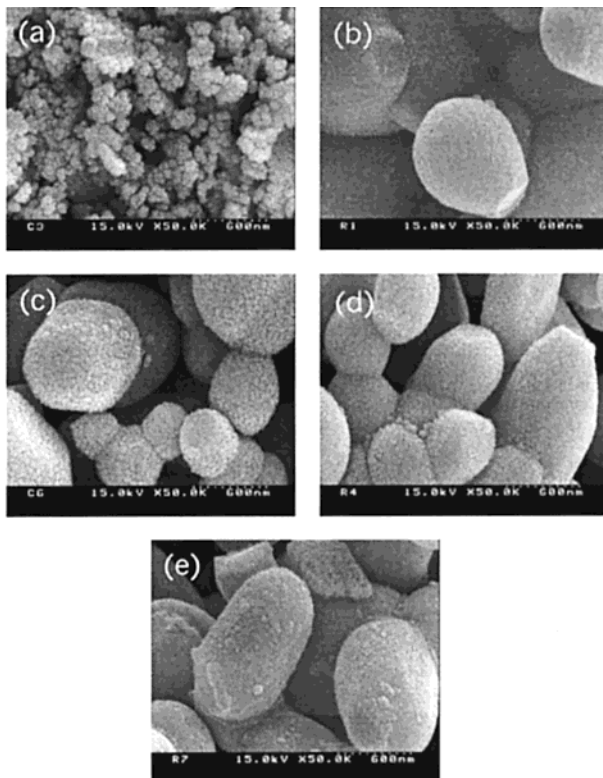


Figure 4. SEM photographs of (a) $\text{Gd}_{1.8}\text{Y}_{0.2}\text{O}_3:\text{Eu}^{3+}$ and Li-doped $\text{Gd}_{1.8}\text{Y}_{0.2}\text{O}_3:\text{Eu}^{3+}$ after firing at 850 °C for 5 h the precursor powder prepared using (b) stoichiometric, (c) 30% excess, (d) 100% excess, and (e) 300% excess amount of Li component.

SEM photographs of the specimens fired at 850 °C for 5 h are compared in Figure 4. No improvement of morphology is observed for $\text{Gd}_{1.8}\text{Y}_{0.2}\text{O}_3:\text{Eu}^{3+}$ phosphor particles before Li doping. On the contrary, well-developed particles are observed in SEM images of Li-doped $\text{Gd}_{1.8}\text{Y}_{0.2}\text{O}_3:\text{Eu}^{3+}$ phosphor. This phenomenon induced in all temperature ranges means that the added Li_2CO_3 makes the particle surface activated by a dissolution of surface area of particulate solids, followed by the formation of well-crystallized particles

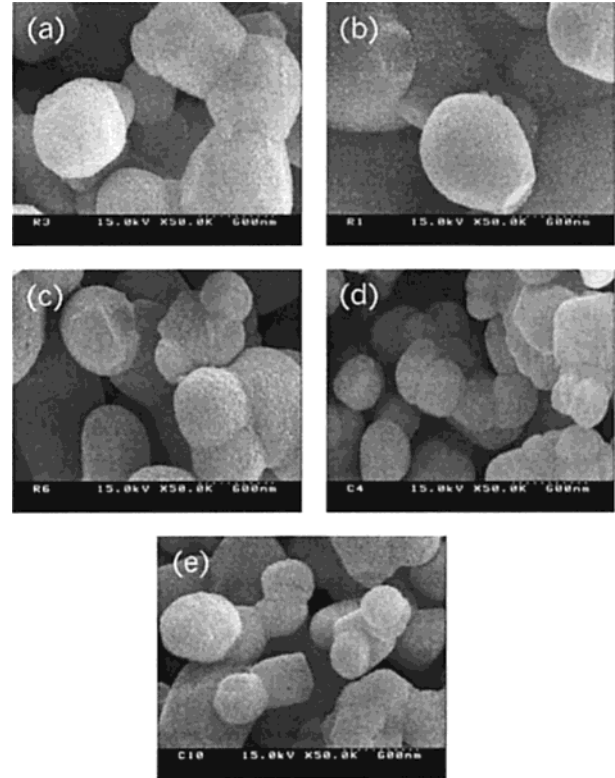


Figure 5. SEM photographs of Li-doped $\text{Gd}_{2-x}\text{Y}_x\text{O}_3:\text{Eu}^{3+}$ with $x =$ (a) 0.0, (b) 0.2, (c) 0.4, (d) 0.6, and (e) 0.8 after firing at 850 °C for 5 h.

with a rounded shape. The phosphor prepared using the stoichiometric amount of Li_2CO_3 shows pseudospherical particles of ~ 500 nm size (Figure 4b). The particle size and roughness of particle surface increase with increasing the excess amount of Li_2CO_3 . The larger particles of elongated sphere shape are obtained when 100% and 300% excess of Li component were added as shown in parts d and e of Figure 4, respectively. Practically, the particles can grow to ~ 3 μm diameter depending on the amount of excess Li_2CO_3 . In this case, unfortunately, it was difficult to improve the particle shape and size distribution. Figure 5 shows the difference in morphology of Li-doped $\text{Gd}_{2-x}\text{Y}_x\text{O}_3:\text{Eu}^{3+}$ as a function of the amount (x value) of substituted Y component upon firing the precursor powder at 850 °C for 5 h. The mean particle size of Li-doped $\text{Gd}_{2-x}\text{Y}_x\text{O}_3:\text{Eu}^{3+}$ phosphor decreases from ~ 500 nm ($x = 0.0$) to ~ 300 nm ($x = 0.8$) with increasing x . These results suggest that the particle size and shape can be controlled by the change of Li or Y contents in Li-doped $\text{Gd}_{2-x}\text{Y}_x\text{O}_3:\text{Eu}^{3+}$ solid-solution at firing temperature lower than 850 °C.

Photoluminescence Spectra. It is known that the Li coactivators, even in very small quantities, frequently play an important role in the enhancement of the luminescent efficiency of phosphors.^{20,21} Indeed, a significantly lower temperature crystallization induced by doping of Li component results in a highly enhanced photoluminescence of $\text{Gd}_{2-x}\text{Y}_x\text{O}_3:\text{Eu}^{3+}$ in this work. Although the mean size of particles is dependent on the amount of added Li during preparation of citrate

(20) Hatayama, T.; Fukumoto, S.; Ibuki, S. *Jpn. J. Appl. Phys., Part 1* **1992**, *31*, 3383.

(21) Lopez, O. A.; McKittrick, J.; Shea, L. E. *J. Lumin.* **1997**, *71*, 1.

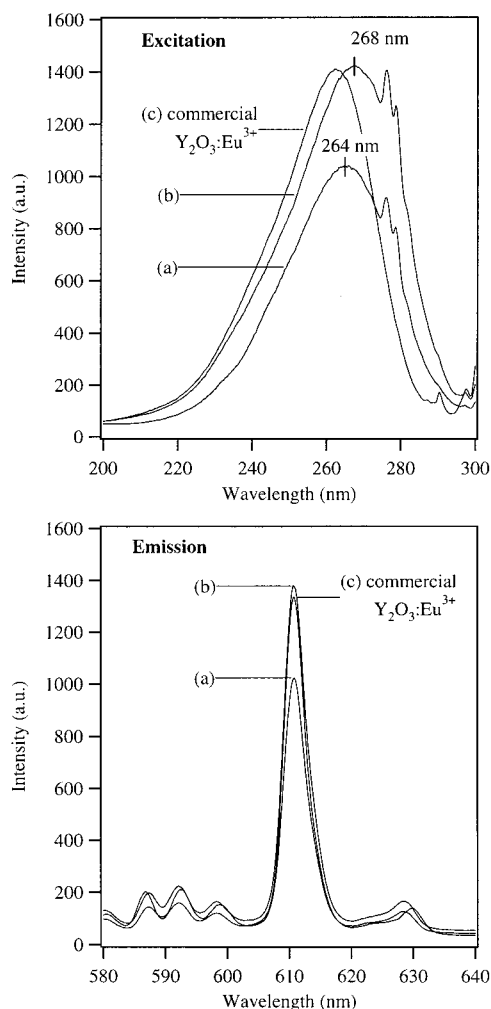


Figure 6. PL excitation (top) and emission (bottom) spectra of (a) $Gd_{1.8}Y_{0.2}O_3:Eu^{3+}$ and (b) Li-doped $Gd_{1.8}Y_{0.2}O_3:Eu^{3+}$ after firing at 650 °C for 5 h and (c) commercial $Y_2O_3:Eu^{3+}$.

precursor, on the other hand, the photoluminescence behavior of Li-doped $Gd_{2-x}Y_xO_3:Eu^{3+}$ showed no strong dependence on the excess amount of Li component at the same firing temperature. Therefore, PL data of the samples prepared by adding 30% excess of Li_2CO_3 are introduced in the present report.

Several repeated measurements of the emission spectra of our solid-solution gave a maximum intensity for the composition of $x = 0.2$. Figure 6 compares PL excitation and emission spectra of commercial $Y_2O_3:Eu^{3+}$ with those of $Gd_{1.8}Y_{0.2}O_3:Eu^{3+}$ and Li-doped $Gd_{1.8}Y_{0.2}O_3:Eu^{3+}$. The broad excitation band around 265 nm is attributed to a charge transfer in the host lattice, and the intense emission at 611 nm is associated with the ${}^5D_0-{}^7F_2$ transition of the Eu^{3+} ion.²² PL excitation and emission intensities of Li-doped $Gd_{1.8}Y_{0.2}O_3:Eu^{3+}$ are much stronger than those of $Gd_{1.8}Y_{0.2}O_3:Eu^{3+}$ before Li doping, as expected. Furthermore, the commercial $Y_2O_3:Eu^{3+}$ phosphor is generally sintered at temperature above 1300 °C. An adoption of hydrolysis technique using urea²³ for the synthesis of $Y_2O_3:Eu^{3+}$ also requires the firing temperature of 1150–1400 °C to achieve an

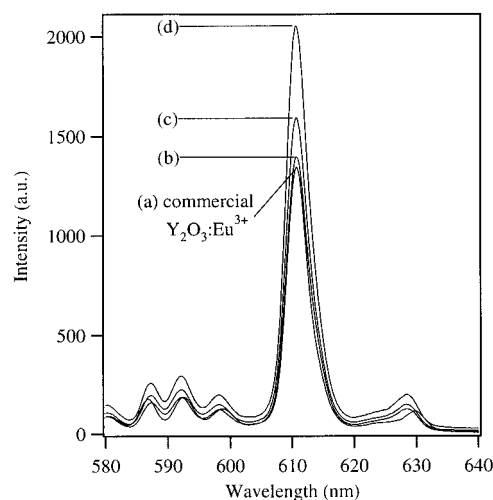


Figure 7. PL emission spectra of (a) commercial $Y_2O_3:Eu^{3+}$ and Li-doped $Gd_{1.8}Y_{0.2}O_3:Eu^{3+}$ after firing at (b) 650, (c) 750, and (d) 850 °C for 5 h.

optimum luminescent property.^{24,25} It is accordingly surprising that the emission intensity of Li-doped $Gd_{1.8}Y_{0.2}O_3:Eu^{3+}$ fired at only 650 °C is comparable with that of commercial $Y_2O_3:Eu^{3+}$. Recently, it was reported that the addition of LiF to $Gd_2O_3:Eu^{3+}$ can increase both its photoluminescence and thermoluminescence, but LiF was supposed to simply act as a lubricant for the complete incorporation of Eu_2O_3 into Gd_2O_3 lattice during the sintering process at 1200 °C.²⁶ However, a red shift of maximum excitation from 264 to 268 nm is observed upon doping of Li component as shown in Figure 6 (top). This shift, coupled with the shift of X-ray diffraction pattern, indicates a change of crystal field around activator ion due to a structural variation of $Gd_{1.8}Y_{0.2}O_3:Eu^{3+}$ by the incorporation of Li^+ ion into the host matrix.

Figure 7 shows the emission intensity of Li-doped $Gd_{1.8}Y_{0.2}O_3:Eu^{3+}$ particles as a function of firing temperature. It is apparent that the relative brightness is enhanced with increasing the firing temperature, the enhancement in emission intensity being close to ~50% when the firing temperature increases from 650 to only 850 °C. Actually, the relative PL intensity is enhanced up to ~70% when the firing temperature increases to 1100 °C. Because of the irregular growth and poor size distribution of phosphor particles, however, the firing temperature range of 650–850 °C was only explored in this work. For comparison, emission intensity measured from a commercial $Y_2O_3:Eu^{3+}$ is also plotted in the figure. It is evidently demonstrated that Li-doped $Gd_{1.8}Y_{0.2}O_3:Eu^{3+}$ powders with mean particle size of 80–500 nm prepared by the citrate route exhibit stronger emission than commercial red phosphor for all firing temperatures. Much higher emission of the sample fired at only 850 °C in this work is an endorsement to the performance.

As shown in Figure 8, strong emissions of Li-doped $Gd_{2-x}Y_xO_3:Eu^{3+}$ around 611 nm are observed in the

(22) Brecher, C.; Samelson, H.; Lempicki, A.; Riley, R.; Peters, T. *Phys. Rev.* **1967**, *155*, 178.

(23) Matijevic, E.; Hsu, W. P. *J. Colloid Interface Sci.* **1987**, *118*, 506.

(24) Jiang, Y. D.; Wang, Z. L.; Zhang, F.; Paris, H. G.; Summers, C. J. *J. Mater. Res.* **1998**, *13*, 2950.

(25) Jing, X.; Ireland, T.; Gibbons, C.; Barber, D. J.; Silver, J.; Vecht, A.; Fern, G.; Trowga, P.; Morton, D. C. *J. Electrochem. Soc.* **1999**, *146*, 4654.

(26) Yeh, S.-M.; Su, C.-S. *Mater. Sci. Eng., B* **1996**, *38*, 245.

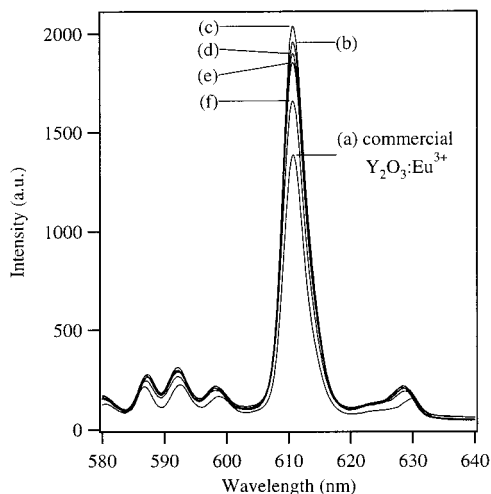


Figure 8. PL emission spectra of (a) commercial $\text{Y}_2\text{O}_3:\text{Eu}^{3+}$ and Li-doped $\text{Gd}_{2-x}\text{Y}_x\text{O}_3:\text{Eu}^{3+}$ with $x =$ (b) 0.0, (c) 0.2, (d) 0.4, (e) 0.6, and (f) 0.8 after firing at 850°C for 5 h.

range of $0.0 \leq x \leq 0.8$ after firing at 850°C for 5 h. The emission intensities of the samples in the range of $0.0 \leq x \leq 0.6$ are particularly higher than that of commercial $\text{Y}_2\text{O}_3:\text{Eu}^{3+}$. Although the maximum brightness is obtained with $x = 0.2$, no significant difference in intensity is observed in such a solid-solution range. Furthermore, the sample of $x = 0.8$ also exhibits more intense emission than commercial red phosphor. When $x \geq 1.0$, the emission intensity considerably decreased, and much higher firing temperature was required to achieve an emission intensity comparable with commercial $\text{Y}_2\text{O}_3:\text{Eu}^{3+}$.

Correlating only particle size (Figures 2–5) to PL behavior (Figures 6–8), the emission intensity of Li-doped $\text{Gd}_{2-x}\text{Y}_x\text{O}_3:\text{Eu}^{3+}$ decreases when the particle size becomes smaller. Such a correlation must result from

a difference in the microstructure of particles. Numerous bulk and surface defects would be expected to exist as a consequence of low-temperature crystallization giving rise to smaller particles and higher surface area of crystallites. Some of these defects may act as non-radiative recombination centers and, therefore, may be responsible for the decrease of the emission intensity observed in smaller particles. Furthermore, the particle size is also dependent on chemical composition. These observations give a conclusion that the optimization of chemical composition and improvement of crystallinity, mean particle size, and dopant distribution are required for the development of more efficient phosphor materials depending on the desired application objectives. Of the most interest to us is that the red emission intensity of Li-doped $\text{Gd}_{2-x}\text{Y}_x\text{O}_3:\text{Eu}^{3+}$ phosphor with $0.0 \leq x \leq 0.8$ is stronger than that of commercial red phosphor regardless of difference in particle size (see Figure 5). Although relative brightness is reduced with decreasing particle size, small particles are preferable when the screen weight is reduced. Higher screen coverage by smaller particles will be able to give greater brightness. Thus, Li-doped $\text{Gd}_{2-x}\text{Y}_x\text{O}_3:\text{Eu}^{3+}$ could be easily processed into diverse types of lamp and display because the most suitable size of spherical particles can be selected depending on the processing condition and required performance. In this respect, our solid-solution system, Li-doped $\text{Gd}_{2-x}\text{Y}_x\text{O}_3:\text{Eu}^{3+}$, appears to be a very promising red phosphor.

Acknowledgment. M.-G. Ko thanks the Ministry of Education for the studentship through the BK21 program. This work was supported by the Ministry of Information and Communication (“Support project of university foundation research ‘00” supervised by IITA).

CM010533M